TISSUE ATTENUATION ESTIMATION BASED ON STANDARD ULTRASONOGRAPHIC DATA

Antonin Misek[1], Jiri Jan[2]

[1]Palacky University Olomouc, Czech Republic (misek@alpha.upol.cz)
[2] University of Technology Brno, Dept. of Biomedical Engineering, Czech Republic (jan@dbme.fee.vutbr.cz)

Abstract **Space-variant ultrasound attenuation in tissue is one of the phenomena that should be taken into account when reconstructing images from ultrasonographic data. This contribution presents a method to estimate automatically one-dimensional attenuation profiles along isolated "rays", forming ultrasonic images. The estimates are based entirely on digital ultrasonographic data, without any reference to a-priori knowledge on anatomical structures involved. Using a standard model of ultrasound propagation, the "layered" and discretised formulation allowed for simplified, thus manageable, least-squares-error estimation of the attenuation profiles. The results of analysing ultrasonographic data obtained from biological objects, as presented on figures, are rather promising.**

Keywords **- ultrasonography, image processing, attenuation maps**

I. INTRODUCTION

Contemporary medical B-mode imaging uses wide-band ultrasonic impulses that are attenuated due to several physical phenomena, when travelling through the imaged tissues. The space-variant and frequency-dependent attenuation should be explicitly taken into account when reconstructing the image to prevent disturbing artefacts. Several papers, e.g. [3-5], have been published on methods of reconstructing the image using a known attenuation map of the imaged area, but a reliable and simple estimation of the attenuation distribution is still a challenging problem. When excluding the approaches based on a-priori known tissue types in the range of the image, the attenuation distribution has to be estimated automatically by analysing the received standard ultrasonic echo, as any other measurements are usually not feasible in clinical routine. The presented contribution introduces a simplifying approach enabling to determine individual attenuation profiles along each image ray from the measured ultrasonographic data automatically, taking into account the properties of ultrasound propagation.

This project has been supported by the grant of the Grant agency of the Czech Republic no. 102/98/1228 and partly also by the grant CEZ MSM 262200011 of the Ministry of Education of the Czech Republic.

II. METHODOLOGY

The sonographic scan-head transmits a wide-band ultrasonic impulse that travels along a straight path (the "ray") with the decreasing wave-amplitude as

$$A(z,f) = A(0,f)e^{-\mu(f,z)z}, \qquad (1)$$

where $A(z,f)$ is the amplitude of the wave component at the frequency f in the distance z from the transducer and $\mu(f,z)$ is the local attenuation coefficient. Let us consider a certain frequency range of the signal, $f \in (f_1, f_2)$, and the propagation with only a single reflection or scattering on each inhomogeneity on the path, thus neglecting any secondary reflections. The ultrasound absorption coefficient is, as in [6], supposed linearly dependent on frequency, $\mu(f) = \mu f$. Constant velocity c of ultrasound propagation in tissue is assumed.

The used model of the imaged tissue is formed as a composition of M homogeneous layers along a ray (fig. 1). Every layer has its constant attenuation coefficient μ_i, its depth Δ_i and its local signal-return-ratio σ_i, produced both by specular reflection and/or backscattering distributed in the layer. If there are specular reflections due to abrupt acoustical impedance changes on the ray trace, the corresponding thin areas are treated as separate layers.

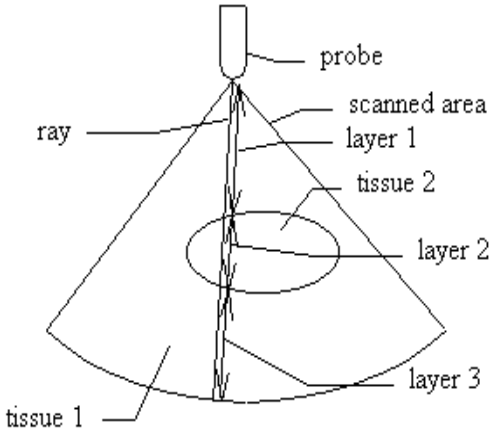

Fig. 1 Schematic example of tissue model

Report Documentation Page

Report Date	Report Type	Dates Covered (from... to)
25 Oct 2001	N/A	-

Title and Subtitle Tissue Attenuation Estimation Based On Standard Ultrasonographic Data	**Contract Number**
	Grant Number
	Program Element Number
Author(s)	**Project Number**
	Task Number
	Work Unit Number
Performing Organization Name(s) and Address(es) Palacky University Olomouc Czech Republic	**Performing Organization Report Number**
Sponsoring/Monitoring Agency Name(s) and Address(es) US Army Research, Development & Standardization Group (UK) PSC 802 Box 15 FPO AE 09499-1500	**Sponsor/Monitor's Acronym(s)**
	Sponsor/Monitor's Report Number(s)

Distribution/Availability Statement
Approved for public release, distribution unlimited

Supplementary Notes
Papers from 23rd Annual International Conference of the IEEE Engineering in Medicine and Biology Society, October 25-28, 2001, held in Istanbul, Turkey. See also ADM001351 for entire conference on cd-rom.

Abstract

Subject Terms

Report Classification unclassified	**Classification of this page** unclassified
Classification of Abstract unclassified	**Limitation of Abstract** UU

Number of Pages
4

The transducer emits a short impulse at time $t = 0$ and then it scans the returning echo. The signal received in time t_1 was obviously reflected/scattered in the tissue in time $\frac{1}{2}t_1$ and it has passed $M(t_1)$ layers, each of them twice, the $M(t_1)$-th layer only to the depth $\frac{1}{2}t_1 c - \sum_{i=1}^{M(t_1)-1}\Delta_i$. It can easily be shown, based on (1), that the amplitude of the echo component at the frequency f is

$$A(z,f) = A(ct/2,f) = A(0,f)\exp\left(-f\sum_{i=1}^{M(t)}\mu_i\tilde{\Delta}_i\right)\sigma_{M(t)}. \quad (1a)$$

On the first look, it may be argued that this expression does not take into account the phase relations among individual returned components of the wave. Nevertheless, according to the problem definition, we are not trying to compensate for the interference, causing e.g. the speckles, but exclusively for the differing attenuation of the signal received at different time instants.

Applying logarithmic transform to (1a), which is always possible as all its components are positive, yields

$$\ln A(z,f) = \ln A(0,f) - f\sum_{i=1}^{M(t)}\mu_i\tilde{\Delta}_i + s_{M(t)} \quad (2)$$

for the interval (f_1, f_2). Here, s_i can be interpreted as a logarithmic measure of the local signal-return-ratio. The primary aim of the analysis is to determine the vector μ but as the only quantity accessible to measurement is $A(z,f)$, all other quantities on the right hand side of (2) must be determined or estimated as well.

When using the (Hilbert-transform derived) envelope of the received wide-band radio-frequency signal, we obtain the resulting integral amplitude of the echo, which can be regarded, on average, approximately proportional to the amplitude mean value with respect to frequency. Working with the mean values removes the frequency dependence from the formulation. Although this approximation may seem to ignore one important aspect, the experimental results support it as a sound simplification, making the problem reasonably tractable. This way, we obtain

$$\int_{f_1}^{f_2}\ln A(z,f)df = \int_{f_1}^{f_2}\left(\ln A(0,f) - f\sum_{i=1}^{M(t)}\mu_i\tilde{\Delta}_i + s_{M(t)}\right)df .$$

Let's denote $y(z) = \int_{f_1}^{f_2}\ln A(z,f)df$ and approximate it by the measured signal value $\ln(A(z))$. After a few simplifying steps and integration we get

$$y(z) = y(0) - \tfrac{1}{2}(f_2^2 - f_1^2)\sum_{i=1}^{M(t)}\mu_i\tilde{\Delta}_i + (f_2 - f_1)s_{M(t)}. \quad (3)$$

Our aim is to estimate μ_i and s_i numerically, utilising the known measurement $y(z)$. The tissue model is initially chosen as a (small) number of layers with corresponding thicknesses $\tilde{\Delta}_i$ and is then automatically refined during the computation thus enabling for arbitrarily complex structure. For the computation, the equation (3), after some modifications, is discretised in z with the space sampling period $\Delta z = cT$, where the time sampling period T is given by the A/D converter of the scanner. The total number N of samples on the ray is therefore fixed while the number M of layers approximating the tissue structure is iteratively updated. After discretisation, the mathematical model acquires the matrix form

$$\mathbf{X}\bar{\mathbf{u}} = \bar{\mathbf{l}}, \quad (4)$$

where

$$\bar{\mathbf{l}} = \begin{bmatrix} y_1 - y_0 + f_3\sum_{i=1}^{M(1)}\mu_{0,i}\tilde{\Delta}_i - f_4 s_{0,M(1)} \\ \vdots \\ y_N - y_0 + f_3\sum_{i=1}^{M(N)}\mu_{0,i}\tilde{\Delta}_i - f_4 s_{0,M(N)} \end{bmatrix}, \qquad \bar{\mathbf{u}} = \begin{bmatrix} f_4\partial\bar{\mathbf{s}} \\ f_3\partial\bar{\boldsymbol{\mu}} \end{bmatrix}$$

($\bar{\mathbf{u}}$ containing the sought corrections $\partial\mu_i$ and ∂s_i to arbitrarily chosen initial estimates $\mu_{0,i}$ and $s_{0,i}$, see [9]) , and

$$\mathbf{X} = \left[\begin{array}{cccc|ccccc} & & & & & & & & \\ & & & & & & & & \\ 1 & 0 & \cdots & 0 & -1 & 0 & 0 & \cdots & 0 \\ 1 & 0 & \cdots & 0 & -2 & 0 & 0 & \cdots & 0 \\ \vdots & \vdots & \ddots & \vdots & \vdots & \vdots & \vdots & \ddots & \vdots \\ 1 & 0 & \cdots & 0 & -\tilde{\Delta}_1 & 0 & 0 & \cdots & 0 \\ \hline 0 & 1 & \cdots & 0 & -\tilde{\Delta}_1 & -1 & 0 & \cdots & 0 \\ 0 & 1 & \cdots & 0 & -\tilde{\Delta}_1 & -2 & 0 & \cdots & 0 \\ \vdots & \vdots & \ddots & \vdots & \vdots & \vdots & \vdots & \ddots & \vdots \\ 0 & 1 & \cdots & 0 & -\tilde{\Delta}_1 & -\tilde{\Delta}_2 & 0 & \cdots & 0 \\ \hline \vdots & \vdots & \ddots & \vdots & \vdots & \vdots & \vdots & \ddots & \vdots \\ 0 & 0 & \cdots & 1 & -\tilde{\Delta}_1 & -\tilde{\Delta}_2 & -\tilde{\Delta}_3 & \cdots & -\tilde{\Delta}_{M(N)} \end{array}\right].$$

Because the size of $\mathbf{X}$ is $N \times 2M$ ($N > 2M$), the equation system is over-determined and can only be solved in the sense of square-error minimisation. According to [8], this estimate is

$$\hat{\bar{\mathbf{u}}} = \left(\mathbf{X}^T\mathbf{X}\right)^{-1}\mathbf{X}^T\bar{\mathbf{l}}. \quad (4a)$$

The details of the iterative algorithm including the initial estimates and the refinement strategy are described in [9].

III. EXPERIMENTAL RESULTS

The designed algorithm has been extensively tested on radio-frequency ultrasonographic data measured on both, a well identifiable tissue-phantom, and a biological in-vivo specimen (pig's heart). The data were scanned with 2964 radio frequency samples on a ray, in the frequency range from 2.5 to 7.5 MHz, and the number of rays in one frame (a fan) was 78.

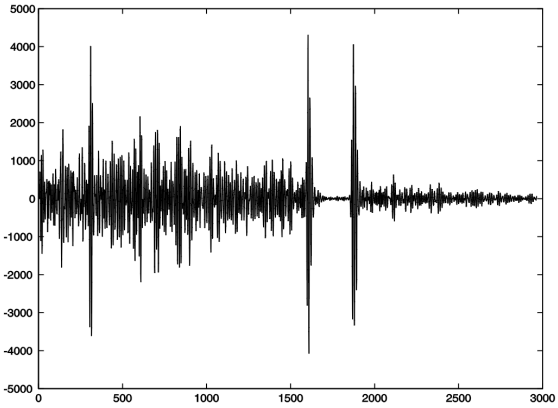

Fig. 2 Measured phantom A-mode signal (detected envelope)

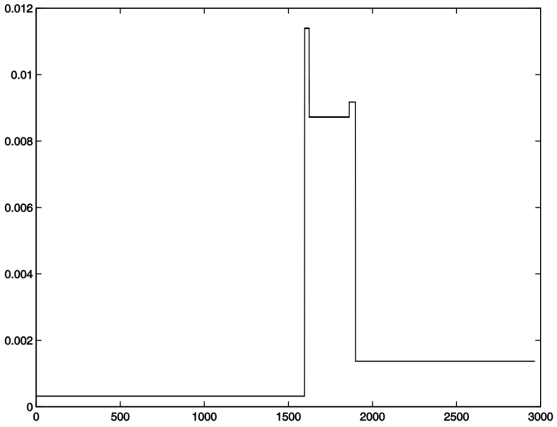

Fig. 3 Estimated attenuation profile $\mu(z)$

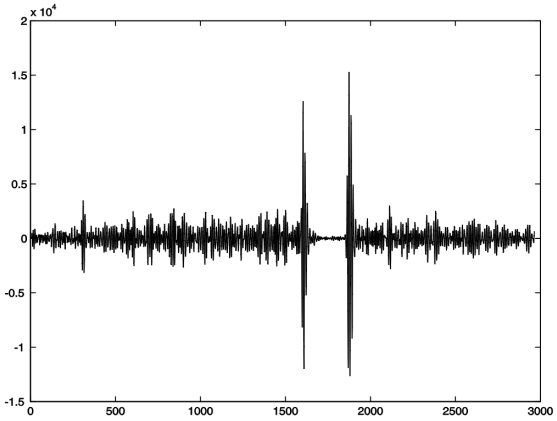

Fig. 4 Restored A-mode signal

Example results of the extensive experimentation are presented on figures. On fig.2, the Hilbert-transform derived signal-envelope along a ray is depicted as an example of input data measured on a phantom. The corresponding attenuation profile derived from the data is presented on fig. 3 and the signal, restored accordingly, on fig. 4.

A scan of a pig's heart (in-vivo) is shown on fig. 5, in video (envelope) signal representation. The attenuation map, as the result of the described computation, utilising the same data as those used for the image fig.5, is presented on fig. 6 (higher brightness represents a higher attenuation).

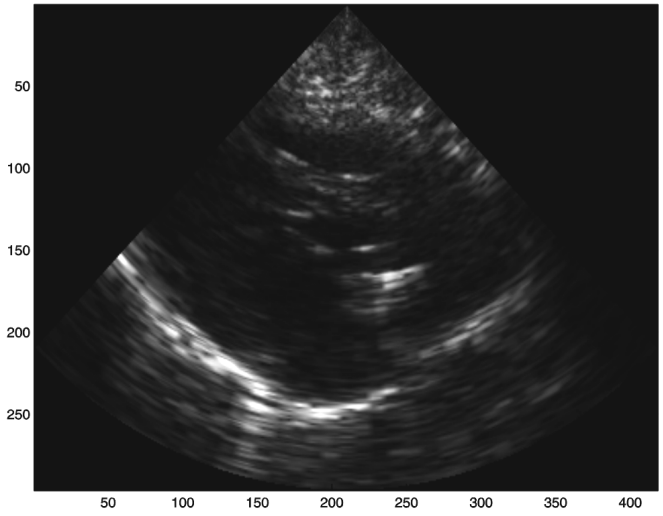

Fig. 5 Ultrasonic image of a pig's heart

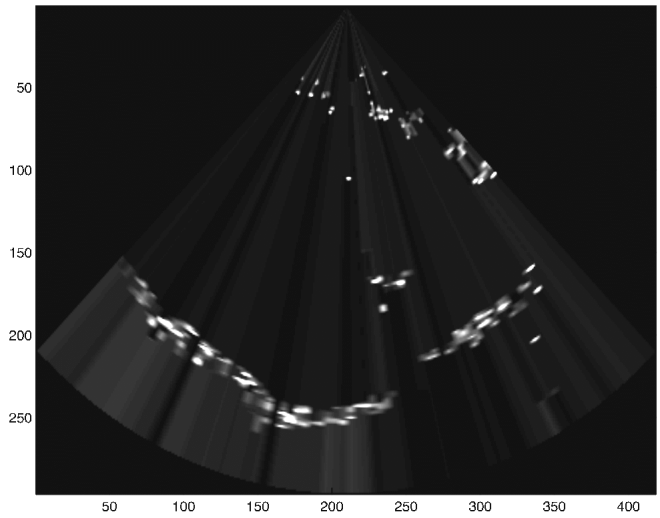

Fig. 6 Computed attenuation map of the object on fig. 5

IV. Conclusions

The suggested method to estimate the ultrasound attenuation map automatically from the measured ultrasonographic data seems to provide a reasonable approximate solution to the given problem, thus forming a step forward on the way to fully automatic attenuation compensation in ultrasonography. The model of ultrasound propagation has been simplified by averaging the frequency dependence and also by neglecting the noise effects, then discretised and the solution sought by the least-square-error method. In spite of the mentioned simplifications, the method has proved to work reasonably well for available sets of test data.

Nevertheless, the independent analysis of individual ray A-mode signals does not take into account the lateral correlation among data in a scan (frame), thus producing some artefacts in the derived maps: the relatively large differences between neighbouring A-mode lines are in some cases rather unrealistic. Therefore, the two-dimensional analysis of the problem, taking into account mutual dependencies among neighbouring rays, is planned as the next step in the project.

Acknowledgement

Authors sincerely acknowledge the contribution of Dr B. Bijnens, Catholic University Leuven (Belgium) who provided valuable measurement data both from a phantom and from in-vivo biological objects.

References

[1] S. Norton, "Reconstruction of a two-dimensional reflecting medium over circular domain," *J. Acoust. Soc. Am.* vol.67, no.4, 1980.

[2] X. Hao, S. Gao, X. Gao, "A novel multiscale nonlinear tresholding method for ultrasonic speckle suppressing," *IEEE Trans. Med. Im.*, vol.18, no.8, 1999.

[3] P. Kilian, B. Bijnens, J. Jan, "Advanced attenuation and frequency shift correction in B-Mode ultrasonic tomography," in *Proc. 18th Annual Int. Conf. IEEE-EMBS*, Amsterdam (The Netherlands) 1996, CD-issue.

[4] P. Kilian, "Digital restoration of ultrasonografic data," PhD theses, Technical University Brno 1999.

[5] P. Kilian, J. Jan, B. Bijnens, "Dynamic filtering of ultrasonic responses to compensate for attenuation and frequency shift in tissues," in *Analysis of Biomedical signals and images (proc. EURASIP conf. BIOSIGNAL 2000)*, pp.261-263, Vutium Brno 2000.

[6] C. R. Hill, *Physical principles of medical ultrasonics*, Chichester (UK) 1986.

[7] J. Jan, *Digital signal filtering, analysis and restoration of signals*, IEE Publ. London (UK) 2000.

[8] A. Bjorck, *Numerical methods for least squares problems*, SIAM, Philadelphia 1996.

[9] A. Misek, J. Jan, "Deriving attenuation profiles from raw digital ultrasonographic data", J. El. Eng. (Ac. Sci. Slovakia), in press.